Nuclear activity and stellar population of a sample of interacting galaxies[*]

M.G. Pastoriza[1,3], C.J. Donzelli[2,3], and C. Bonatto[1]

[1] Departamento de Astronomia, IF-UFRGS, C.P. 15051, CEP 91501-970, Porto Alegre, RS, Brazil
[2] IATE, Observatorio Astronômico, Universidad Nacional de Córdoba, Laprida 854, 5000, Córdoba, Argentina
[3] Visiting Astronomer at CASLEO Observatory

Abstract. In this paper we investigate the nuclear activity and stellar population in a sample of 27 physical galaxy pairs. Equivalent widths of absorption features are used to characterise the nuclear stellar population according to templates: most galaxies of the sample have important flux contributions from stars younger than 10^8 years. According to classical diagnostic-diagrams the galaxies in our sample are either classified as H II regions or have emission line ratios near the transition zone between H II regions and LINERs. Based on the observed spectra, only 4 galaxies show LINER properties and 1 nucleus is a Seyfert 2. We found that the spectrum of a transition object (38% of the sample) can be described by a combination of an AGN with an H II region. As a result, 20 galaxies of the present sample may host a low-luminosity active nucleus.

Key words: galaxies: active – galaxies: interactions – galaxies: nuclei – galaxies: stellar content

1. Introduction

In a recent paper, Donzelli & Pastoriza (1997, hereafter DP97) have studied the spectroscopic properties of 27 physical pairs consisting of a main galaxy (component A) and a companion (component B) which has about half or less the diameter of component A. We confirmed for this sample an earlier result that physical pairs have higher mean star formation rates than isolated galaxies (Bushouse 1986; Kennicutt et al. 1987). However, it was not found the excess of AGN which was reported in previous studies of similar galaxy samples (e.g. Keel et al. 1985; Veilleux, Kim & Kron 1995; Liu & Kennicutt 1995). In fact, we found in our sample of 54 galaxies only 4 LINER and 1 Seyfert 2 nuclei, which represent 9.2% of the sample. In a recent paper Ho, Filippenko & Sargent (1997) show that in a magnitude-limited sample of 486 galaxies with $B_T \leq 12.5$,

half of the objects have H II star-forming nuclei, and the other half have some form of AGN or composite spectrum.

Enhancement of the star formation activity in interacting galaxies, like that observed in the physical pairs of our sample, can be accounted for by merger between a gas-rich disk and a less-massive dwarf galaxy (Hernquist & Mihos 1995). As a consequence of the interaction, the disk gas is forced to fall into the inner regions of the disk. The gas accumulates in the nuclear region forming high-density knots. Intense star formation can take place in these condensations, which can be identified as those observed in galaxies with circumnuclear star formation like NGC 613, NGC 1672 and NGC 1097 (Sersic & Pastoriza 1967; Osmer, Smith & Weedman 1974). The circumnuclear star-formation can mask a low luminosity LINER or even a Seyfert 2 nucleus (e.g. Storchi-Bergmann, Wilson & Baldwin 1996b; Philips, Charles & Baldwin 1983).

Recently Veron, Goncalves & Veron-Cetty (1997, hereafter V97) reported a number of galaxies having composite spectra. When observed with projected apertures larger than 2 kpc, these galaxies show spectra intermediate between those of an H II region and an **AGN**, due to the simultaneous presence on the slit of a Seyfert or LINER nucleus and an H II region. In this paper we argue that the observed deficiency of Seyfert nuclei in the DP97 sample, as compared to Liu & Kennicutt (1995) sample, might be explained by a masking of the **AGN** spectrum by strong circumnuclear star formation activity.

The goal of this work is to study the stellar population and nuclear emission in the sample of 27 physical galaxy pairs presented in DP97. The galaxy sample and observations are presented in Sect. 2. The nuclear stellar population is analyzed in Sect. 3. In Sect. 4 we subtract the stellar population templates from the galaxy spectra in order to obtain pure-emission line ratios; diagnostic-diagrams are used to classify the emission line spectra. In Sect. 5 the nature of the composite spectra is studied. Conclusions are summarised in Sect. 6.

2. Galaxy sample

The analyses have been carried out using optical spectra in the range 3700—7000 Å of the following objects: *(i)* the interacting galaxies presented in DP97; *(ii)* the Seyfert 1 J 15.22 (Maza et

Fig. 1. Interacting pair AM 2238-575 A and B. North is up and East left. Scale is $10' \times 10'$. Image taken from Digital Sky Survey (DSS).

Fig. 2. Interacting pair AM 2322-821 A and B. North is up and East left. Scale is $10' \times 10'$. Image taken from Digital Sky Survey (DSS).

al. 1994); *(iii)* the classical Seyfert 2 NGC 1068; *(iv)* the LINER AM 2054-433S (Donzelli & Ferreiro 1998); and *(v)* the H II regions R5, R10 and R1 of the Gumm 38a H II region complex, which show different states of excitation and have solar metallicity (Girardi et al. 1997, hereafter G97).

Spectra of the interacting galaxies, the LINER AM 2054-433S, and the Seyfert 1 J 15.22 were obtained with the REOSC Spectrograph with a Tektronix 1024×1024 CCD, at the 2.25m Ritchey-Chretien telescope of CASLEO, San Juan, Argentina. The galaxies were observed using a slit $2.5'$ long and $3''$ wide in the spectral range 3700—7000 Å, with spectral resolution of 3.3 Å. NGC 1068 and the Gumm 38a H II region complex were observed at the CTIO 1.0m telescope. The spectrograph plus 2D-Frutti detector provided spectra in the range 3700—7000 Å with a resolution of 7 Å; the slit length corresponds to $5.2'$. We assume throughout this paper $H_O = 75\,\mathrm{km\,s^{-1}\,Mpc^{-1}}$.

Additional details on the observation and data reduction, as well as reddening and radial velocity corrections can be found in DP97 for the interacting galaxies, and in G97 for the Gumm 38a H II region complex. Radial velocity and reddening for NGC 1068 were taken from RC3 (de Vaucouleurs et al. 1991); for J 15.22 and AM 2054-433S, the radial velocities were measured in the observed spectra, and the reddenings were interpolated from nearby galaxies (values taken from RC3). Typical examples of the interacting pairs of our sample are shown in Figs. 1 and 2.

3. Absorption line spectra

The characterisation of the stellar population of the interacting galaxies is based on the equivalent widths (**EW**s) of the more prominent absorption features, i.e., Ca II$_{\lambda 3933}$, CN$_{\lambda 4200}$, CH G band, and Mg I$_{\lambda 5175}$. We have also measured additional absorption features and the flux contribution at $\lambda 4600$ Å and $\lambda 5300$ Å for those galaxies in which the population template selection was difficult. These data are presented in Table 1 for both components of the interacting pairs. Previous to the measurements, all spectra were normalised to the continuum at $\lambda 5870$ Å where the flux contribution from young stellar populations is less than 2% (Bica 1988). Typical errors are $\approx 15\%$ for **EW** ≥ 10 Å and somewhat higher ($\approx 20\%$) for **EW** ≤ 5 Å. Continuum tracing and spectral windows are those defined by Bica & Alloin (1986). The **EW**s were used to classify the spectrum of each galaxy in terms of Bica's (1988) templates, which span the properties of the more usual nuclear stellar populations observed in normal galaxies. The basic characteristics of the templates can be summarised as follows: E1—E3 and S1—S3 are red stellar populations with metallicity decreasing from 4 to 1 times solar. S4—S7 is a sequence of increasing contributions from blue components: S4 contains 10% of flux contribution at $\lambda 5870$ Å from populations younger than 1 Gyr, while S7 contains 80%.

The resulting frequency of stellar population templates for each component of our sample pairs is shown in Fig. 3. The histogram shows an excess of blue stellar population templates for the B components with respect to the A components. In fact 55% of the B components have S5 to S7 stellar population types, while $\approx 37\%$ of the A components have blue stellar population types. This result reveals intrinsic differences between the stellar populations of both components of the galaxy pairs, but it might also be related to the size of the observed region. In fact, the average major diameter of the B components is $\approx 12''$, and since the spectra have been extracted from a rectangular aperture of
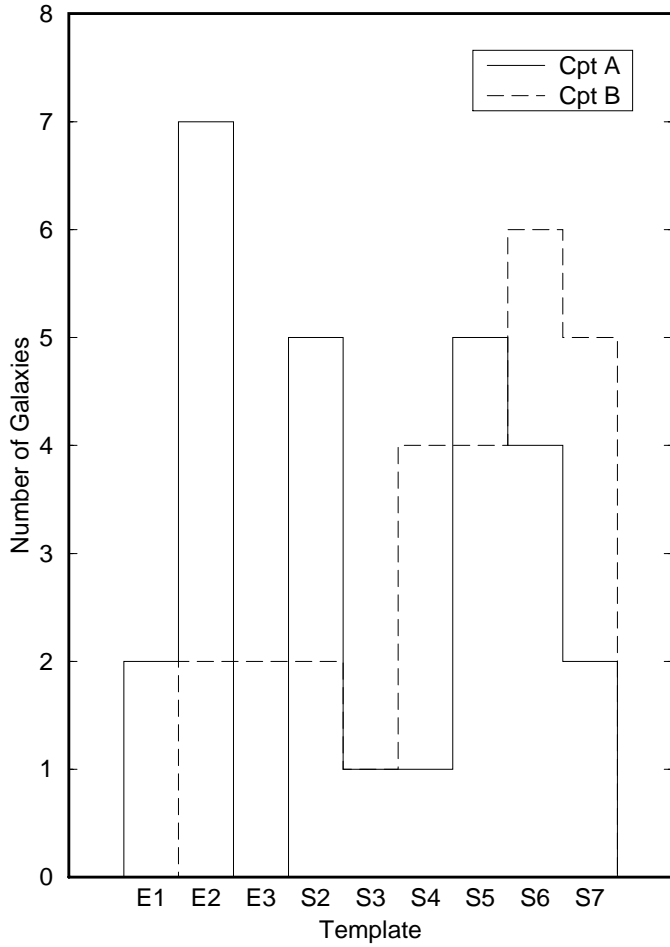
Fig. 3. Frequency of stellar population templates in the sample galaxies

torted late-type spirals, except AM 0821-783B, AM 1254-321B and AM 1256-433 which probably are early-type galaxies.

The frequency of stellar population templates in the sample galaxies (Fig. 3) shows that most of these galaxies have an important flux contribution from stars younger than 10^8 years. V-band luminosity and the corresponding mass fraction for a selection of E1—S7 galaxy stellar population models have been computed by Bica, Arimoto & Alloin (1988) which show that recent star formation (S1—S6 templates), although very important in V flux, has a negligible contribution (less than 5%) in mass. For the S7 template, the contribution from young stars to the observed light at $\lambda 5870\,\text{Å}$ amounts to more than 80%, and its mass contribution (about 15%) becomes important.

As remarked by Bica, Arimoto & Alloin (1988), early-type galaxies with recent star-formation (E7 and E8 templates) require some mechanism of external gas injection such as, for example, interaction and/or merger. In our sample there are examples of early-type galaxies interacting with star-forming galaxies (e.g. AM 1224-331, AM 2330-451 and AM 2105-332) whose stellar population is described by the E1, E2 or E3 templates – which do not present recent star formation. This could mean that there was no gas transfer between both components.

4. Emission lines and diagnostic diagrams

After reddening and radial velocity corrections, the corresponding stellar population template (Table 1) was subtracted from each spectra of the galaxy sample. This procedure is illustrated in Fig. 4 for a red (E2) and a blue (S5) stellar population cases. This figure shows the observed spectra, the corresponding stellar population templates and the resulting pure emission spectra of the interacting galaxies AM 2238-575A and AM 2322-821B.

Emission line fluxes were measured on the pure emission spectra and were reddening corrected using the expression (12) of McCall, Rybski & Shields (1985), which should take into account any residual underlying stellar absorption, and which is based on the $1/\lambda$ extinction law of Schild (1977). On the other hand, we caution that extragalactic reddening laws for extended objects seem to work differently than interstellar ones deduced from stars (Calzetti, Kinney & Storchi-Bergmann, 1994; Calzetti et al., 1995). However, the Calzetti extragalactic obscuration law follows very closely the $1/\lambda$ law in the visual spectral range, and significant differences arise only in the ultra-violet (Bonatto et al. 1999). The internal extinction for each galaxy was also taken into account assuming an intrinsic Hα/Hβ ratio of 2.85 which corresponds to the case B Balmer recombination in an optically thin plasma at T $= 10^4\,^o$K (Osterbrock 1989). We estimate an rms of 0.06 magnitudes for residuals of the system sensitivity function fitting. Nevertheless, errors in the fluxes are about 15% due to inaccuracies in the continuum subtraction and deblending technique. The corresponding emission line ratios for both components of the galaxy pairs are listed in Table 2.

Usually, diagnostic-diagrams with emission line ratios of easily observed lines are employed to classify the spectra of extragalactic objects according to the main excitation mechanisms. Unfortunately, due to border effects we could not use

$3'' \times 3''$, the bulge and part of the disk of the B components have been observed. On the other hand, for the A components, which have an average major diameter larger than 1.5', only the central region was observed.

The stellar population analysis shows that: *(i)* nearly half of the A component bulges have a red stellar population (E1, E2 and S2 templates), and thus typical young stars are absent in the nuclear region of these galaxies. In Fig. 4 (top panel) we show the observed spectrum of AM 2238-575 A along its E2 stellar population template. Notice that this is a case of an Sc galaxy (Fig. 1) with a very red bulge. The remaining A components exhibit an appreciable flux contribution from young stars (S4—S7 templates) at the normalisation wavelength $\lambda 5870\,\text{Å}$. In the bottom panel of Fig. 4 we show the spectrum of AM 2322-821 B together with its blue S5 stellar population template; *(ii)* more than 70% of the B components have a strong flux contribution from stellar populations younger than 10^8 years (S4—S7 templates). Intense star formation occurs on the main body of the weaker component of the pairs; *(iii)* due to the small apparent diameter of these B components and the tidal distortion of their main body, it is very difficult to classify them according to morphological type. Thus, from the stellar population analysis we infer that most of these galaxies are gas-rich irregulars or dis-

Table 1. Equivalent widths for the galaxy sample

Galaxy	EW (Å)					template
	CaII	CN	CH	FeI	MgI	
AM 0103-302A	2	2	4	1	6	S6
AM 0103-302B	8	1	3	–	2	S4
AM 0134-373A	2	3	4	2	3	S6
AM 0134-373B	4	5	7	2	4	S5
AM 0304-391A	16	13	9	2	10	E1
AM 0304-391B	20	14	10	1	6	S3
AM 0728-664A	–	–	–	2	8	S2
AM 0728-664B	–	–	–	–	4	S7
AM 0821-783A	–	–	–	2	9	E2
AM 0821-783B	12	6	8	5	6	E3
AM 0905-232A	–	–	–	–	9	E2
AM 0905-232B	–	–	–	–	–	–
AM 0907-753A	–	–	–	–	7	S5
AM 0907-753B	–	–	–	–	5	S7
AM 1116-290A	–	–	–	2	6	S5
AM 1116-290B	–	–	–	3	6	S6
AM 1118-350A	–	–	2	1	4	S7
AM 1118-350B	–	–	3	–	5	S7
AM 1127-351A	–	–	–	2	5	S6
AM 1127-351B	–	–	–	1	2	S2
AM 1219-430A	6	5	5	1	6	S5
AM 1219-430B	2	10	3	1	2	S6
AM 1224-331A	15	10	9	2	5	E2
AM 1224-331B	12	6	4	1	3	S6
AM 1252-443A	–	–	–	2	6	S5
AM 1252-443B	–	–	–	–	3	S7
AM 1254-321A	–	–	–	–	9	E2
AM 1254-321B	–	–	–	–	10	E2
AM 1256-433A	13	13	10	2	10	E2
AM 1256-433A*	18	15	9	–	–	S2
AM 1256-433B	19	10	9	4	7	E2
AM 1256-433B*	–	–	–	–	–	S5
AM 1304-333A	–	–	–	3	5	S6
AM 1304-33B	–	–	–	4	4	S4
AM 1401-324A	–	7	2	–	2	S2
AM 1401-324B	–	–	–	–	5	S4
AM 1448-262A	–	–	–	–	8	S3
AM 1448-262B	–	–	–	–	2	S7
AM 2030-303A	7	10	6	1	6	S2
AM 2030-303B	16	17	7	3	6	S2
AM 2058-381A	12	17	11	4	8	S2
AM 2058-381B	–	–	3	2	6	S6
AM 2105-332A	18	11	9	2	9	E2
AM 2105-332B	12	8	7	2	4	S4
AM 2229-735A	4	–	4	2	3	S5
AM 2229-735B	5	6	5	3	6	S6
AM 2238-575A	15	7	8	1	8	E2
AM 2238-575B	14	8	9	2	6	E3
AM 2306-721A	–	7	9	1	1	S7
AM 2306-721B	–	–	–	–	4	S6
AM 2322-821A	11	6	8	3	4	S4
AM 2322-821B	–	2	4	3	2	S5
AM 2330-451A	18	13	11	4	9	E1
AM 2330-451B	10	9	12	6	7	S5

Table Notes. Column (7) gives the stellar population template derived from the **EW**s.

[OII]$_{\lambda 3727}$, which restricted the number of diagnostic-diagrams available for the analysis.

The classical (Veilleux & Osterbrock 1987) diagnostic-diagrams [OIII]$_{\lambda 5007}$/Hβ × [NII]$_{\lambda 6584}$/Hα and [OIII]$_{\lambda 5007}$/Hβ × [SII]$_{\lambda\lambda 6717,6731}$/H$\alpha$, are shown in the upper and lower panels of Fig. 5, respectively. These diagrams are divided in three zones corresponding to the different degrees of activity in the nucleus. Nuclear H II regions and starburst galaxies lie to the left of the solid line, while Seyferts and LINERS are located to the right of this line, with the Seyferts presenting larger values of [OIII]$_{\lambda 5007}$/Hβ. The solid line in Figs. 5 and 6, which separates H II regions from AGN, has been adapted from Veilleux & Osterbrock (1987). The consistency of this curve as a true boundary between these two types of objects has been checked with the photoionisation models of Rola et al. (1997) for the diagnostic-diagrams used in the present paper. We noticed that their hottest model (corresponding to the extreme H II regions) matches very well the separating line adopted in the present work.

Fig. 5 shows that the line ratios of most of the interacting galaxies fall in the zone of H II region spectra. However, some of these are very near the transition zone between H II regions and LINERs. In fact, in the [OIII]$_{\lambda 5007}$/Hβ × [OI]$_{\lambda 6300}$/Hα diagnostic-diagram, which is a good indicator of galaxies with LINER emission line spectrum (Fig. 6), 4 galaxies have line ratios typical of LINERs and 1 is probably a Seyfert 2, which represents 9.2% of the total sample.

Although some line-ratios indicate the presence of an AGN, broad components in emission lines have not been detected in the present spectra, suggesting that the AGN might be a very low-luminosity source, heavily contaminated by the H II region emission.

5. Composite spectra

As it was found in the previous section, only 4 galaxies could be classified as LINERs and 1 as Seyfert 2 in at least one of the diagnostic-diagrams, but several galaxies are in the transition zone. These transition objects could have a composite spectrum due to the simultaneous presence on the slit of a Seyfert nucleus and an H II region (V97). In order to test this hypothesis we have built composite spectra, combining emission-pure spectra of a typical Seyfert 1 (J 15.22), Seyfert 2 (NGC 1068) and LINER (AM 2054-433S) with the H II region spectra of solar abundance R1a, R5a and R10a, of the Gumm 38a complex. These galactic H II regions have been selected because they are as metallic as the circumnuclear H II regions of nearby galaxies (Storchi-Bergmann et al. 1996a), are purely photoionised by stars, and also show a wide range of excitation (G97). For J 15.22 and NGC 1068, suitable stellar population templates were also subtracted following the method described in Sect. 3.

The composite spectra were built adding different fractions of the H II region spectrum to that of the **AGN**. To do this, the stellar-population subtracted AGN and H II region spectra have been normalised at the peak of the [OIII]$_{\lambda 5007}$ emission line. This process is illustrated in Fig. 7, in which we combine 30%

Table 2. Reddening-corrected emission line ratios

Galaxy	E(B-V)	$\log \frac{[OIII]}{H\beta}$	$\log \frac{[OI]}{H\alpha}$	$\log \frac{[NII]}{H\alpha}$	$\log \frac{[SII]}{H\alpha}$	Type
AM 0103–302A	0.84	-0.08	-0.98	-0.31	-0.57	CS
AM 0103–302B	–	–	–	-0.54	-0.37	
AM 0134–373A	0.70	-0.33	-1.56	-0.44	-0.73	RH II
AM 0134–373B	1.10	-0.23	-1.45	-0.35	-0.58	CS
AM 0304–391A	–	–	–	1.04	–	
AM 0304–391B	–	–	–	-0.12	–	
AM 0728–664A	–	–	–	-0.12	–	
AM 0728–664B	0.07	-0.44	–	-0.38	-0.46	CS
AM 0821–783A	–	–	–	–	–	NE
AM 0821–783B	–	–	–	–	–	NE
AM 0905–232A	–	–	–	–	–	NE
AM 0905–232B	–	–	–	–	–	
AM 0907–753A	1.33	0.36	–	-0.41	-0.69	CS
AM 0907–753B	–	–	–	-0.37	-0.23	
AM 1116–290A	1.44	0.16	-0.65	-0.23	-0.42	CS
AM 1116–290B	0.84	–	–	-0.56	-0.43	
AM 1118–350A	0.43	-0.51	–	-0.49	-0.63	CS?
AM 1118–350B	0.48	-0.51	-1.48	-0.44	-0.64	CS
AM 1127–351A	0.48	-0.10	–	-0.46	–	
AM 1127–351B	0.26	0.24	–	-0.93	-0.59	CS?
AM 1219–430A	1.19	-0.46	–	-0.63	-1.18	RH II
AM 1219–430B	0.64	-0.63	-1.05	-0.56	-0.75	RH II
AM 1224–331A	–	–	–	–	–	NE
AM 1224–331B	0.72	0.32	-1.40	-1.15	-0.59	CS
AM 1252–443A	0.94	–	–	-0.41	-0.75	
AM 1252–443B	0.06	-0.09	–	-0.73	–	RH II
AM 1254–321A	–	–	–	–	–	NE
AM 1254–321B	–	–	–	–	–	NE
AM 1256–433A	–	–	–	–	–	NE
AM 1256–433A*	0.83	0.20	-1.17	-0.36	-0.39	CS
AM 1256–433B	–	–	–	–	–	NE
AM 1256–433B*	–	–	–	-0.54	-0.19	
AM 1304–333A	0.55	-0.40	–	-0.37	-0.51	CS
AM 1304–333B	1.00	-0.55	-1.41	-0.37	-0.53	CS
AM 1401–324A	–	–	–	-0.30	-0.42	
AM 1401–324B	–	–	–	-0.46	-0.32	
AM 1448–262A	–	–	–	–	–	NE
AM 1448–262B	0.35	0.10	–	-0.72	-0.48	CS?
AM 2030–303A	–	–	–	-0.46	-0.40	
AM 2030–303B	0.43	-0.03	–	-0.89	-0.52	CS?
AM 2058–381A	–	–	–	-0.33	-0.23	
AM 2058–381B	0.69	0.52	-1.07	-1.12	-0.36	CS
AM 2105–332A	–	–	–	–	–	NE
AM 2105–332B	0.96	–	–	-0.64	-0.46	
AM 2229–735A	0.58	0.04	–	-0.68	-0.57	CS?
AM 2229–735B	0.34	0.08	–	-0.40	-0.43	CS
AM 2238–575A	–	–	–	–	–	NE
AM 2238–575B	–	–	–	–	–	NE
AM 2306–721A	0.32	0.17	-1.31	-0.59	-0.38	CS
AM 2306–721B	–	–	–	-0.26	-0.45	
AM 2322–821A	0.25	-0.23	-1.07	-0.32	-0.22	CS
AM 2322–821B	0.11	0.16	-1.38	-0.68	-0.39	CS
AM 2330–451A	–	–	–	–	–	NE
AM 2330–451B	–	–	–	-0.1	-0.49	

Table Notes. CS – composite spectrum (**AGN** + H II region); RH II –
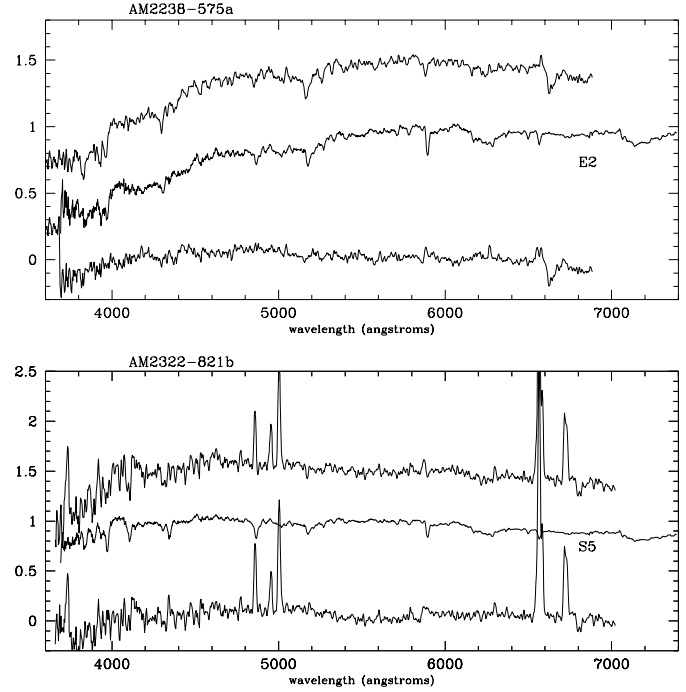pure H II region spectrum; NE – no emission spectrum.

Fig. 4. Spectra of the galaxies AM 2238-575A (top) and AM 2322-821B (bottom). The corresponding templates and the resulting pure-emission spectra are also shown. Constants have been added to the spectra for ease of visualisation.

of the spectrum of the Seyfert 1 J 15.22 with 70% of the moderate excitation H II region R 10a. As a result, the H II region spectrum masks that of the Seyfert 1, leaving only a slight broadening at the base of Hα and Hβ.

The resulting emission line ratios of the composite spectra are plotted in the diagnostic-diagrams (long dashed lines) in Figs. 5 and 6, where the effect of the H II region contamination can be seen: for the composite model shown in Fig. 7, the 70% H II region contribution shifts the line ratios of the Seyfert 1 to the typical H II region zone. In terms of [OIII]$_{\lambda5007}$ flux, this H II region fraction corresponds to 64% of the total, a reasonable amount for low luminosity nuclei. Indeed, in the moderate star-forming galaxy NGC 1097, the contribution of a few individual H II regions in the ring around the nucleus to the total [OIII]$_{\lambda5007}$ nuclear flux is $\approx$50% (Storchi-Bergmann, Wilson & Baldwin 1996b). A more dramatic example is NGC 3310 in which the H II region contribution amounts to $\approx$90% (Pastoriza et al. 1993).

In order to check if the selection of H II regions with different properties would affect the results, we calculated using the CLOUDY code (Ferland 1993), a series of H II region models photoionised by black-body spectra with effective temperatures T=35 000K, 40 000K and 50 000K. Since we are dealing with circumnuclear H II regions, and the low spectral resolution prevents a direct calculation of the electron density (N_e) from the [SII]$_{\lambda\lambda6717,6731}$ lines, we have adopted the average value obtained for the circumnuclear H II regions observed in NGC 3310 (Pastoriza et al. 1993), i.e. $N_e = 500\,\mathrm{cm}^{-3}$. The Hydrogen gas
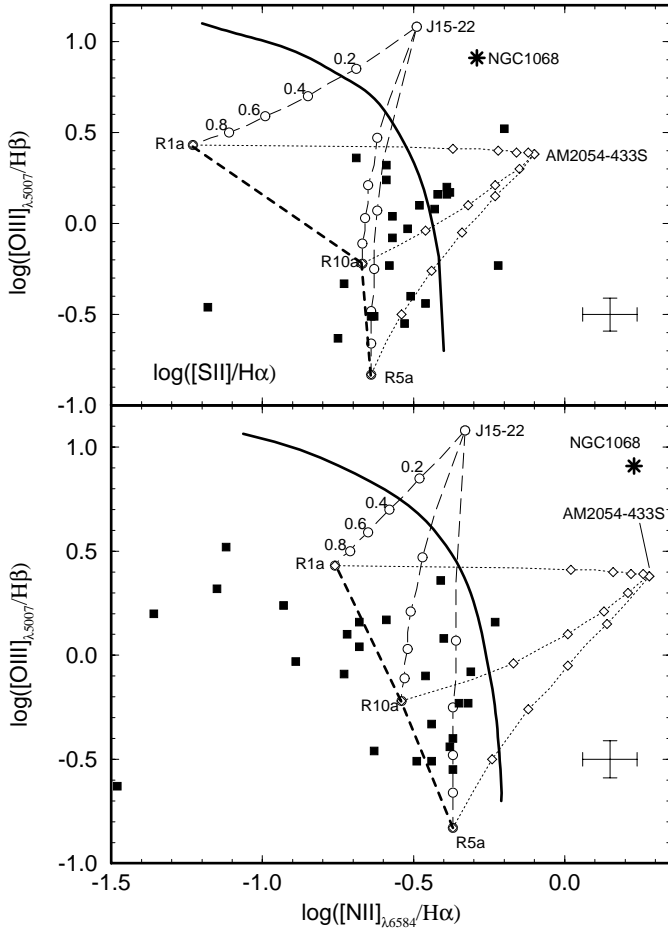
Fig. 5. Top panel: [OIII]$_{\lambda5007}$/Hβ × [SII]$_{\lambda\lambda6717,6731}$/H$\alpha$. The long-dashed lines indicate the effect on the line ratios due to the "contamination" of the Seyfert 1 spectrum (J 15.22) with the H II region spectra R1a, R10a and R5a. The H II region contributions (at $\lambda5007$ Å) are indicated. Corresponding models for the LINER AM 2054-433S are shown as empty diamonds. The heavy solid line represents the "classical" boundary between H II regions (left), LINERS (right) and Seyferts (top right). Filled squares are the line ratios measured in our sample galaxies. The heavy-dashed line marks off the locus of metallic H II regions. The location of NGC 1068 is indicated. Bottom panel: same as above for [OIII]$_{\lambda5007}$/Hβ × [NII]$_{\lambda6584}$/Hα. Typical error bars are shown.

density was fixed at $500\,\mathrm{cm^{-3}}$, and models were calculated for solar[1] and half-solar metallicity, and ionisation parameter in the range $-2.5 \leq U \leq -3.5$. The T=50 000K and solar metallicity models for the [OI]$_{\lambda6300}$/Hα × [OIII]$_{\lambda5007}$/Hβ diagram are shown in Fig. 6. The use of models with the same range of U and lower abundances would shift the H II region loci further to the left, increasing the number of **AGN** candidates among the galaxies of our sample.

---

[1] Solar abundances (by number), with respect to Hydrogen: He $= 9.80 \times 10^{-2}$, C $= 3.63 \times 10^{-4}$, N $= 1.12 \times 10^{-4}$, O $= 8.51 \times 10^{-4}$, Ne $= 1.23 \times 10^{-4}$, Na $= 2.10 \times 10^{-6}$, Mg $= 3.80 \times 10^{-5}$, Al $= 2.95 \times 10^{-6}$, Si $= 3.55 \times 10^{-5}$, S $= 1.62 \times 10^{-5}$, Ar $= 3.63 \times 10^{-6}$, Ca $= 2.29 \times 10^{-6}$, Fe $= 4.68 \times 10^{-5}$ and Ni $= 1.76 \times 10^{-6}$.
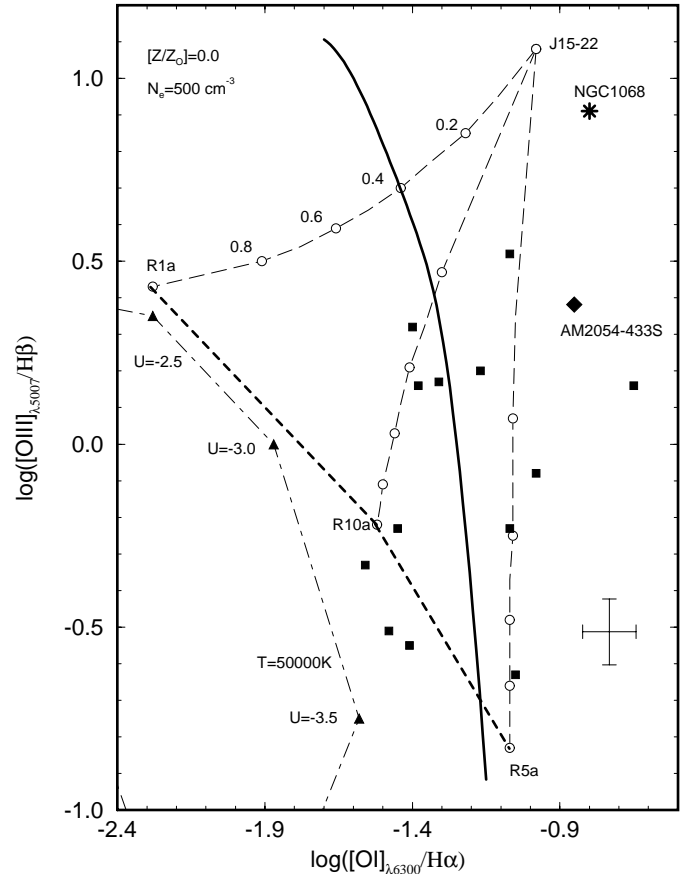
Fig. 6. Same as Fig. 5 for the line ratios [OIII]$_{\lambda5007}$/Hβ × [OI]$_{\lambda6300}$/Hα. The dot-dashed line indicates the H II region models calculated for effective temperature T=50 000 K, electron density $N_e = 500\,\mathrm{cm^{-3}}$, ionisation parameter in the range $-2.5 \leq U \leq -3.5$, and solar metallicity.

From Figs. 5 and 6, all the points to the right of the Gumm 38a H II regions (heavy-dashed line) can be reproduced by a combination of an **AGN** spectrum with that of an H II region. In this sense, only the points to the left of that line would be pure H II regions. Notice that for our sample galaxies, the [OI]$_{\lambda6300}$ and [SII]$_{\lambda\lambda6717,6731}$ lines are more sensitive indicators of the presence of a composite spectrum than [NII]$_{\lambda6584}$. Indeed, in the [NII]$_{\lambda6584}$/Hα diagnostic-diagram (Fig. 5, bottom panel), 50% of the line ratios appear to be from composite spectra, whereas in the [SII]$_{\lambda\lambda6717,6731}$/H$\alpha$ (Fig. 5, top panel) and [OI]$_{\lambda6300}$/Hα (Fig. 6) diagrams, this fraction increases to $\approx$78%.

Taking into account the position of the observed line ratios with respect to the Gumm 38a H II regions zone in the 3 diagnostic-diagrams (Figs. 5 and 6), we give in column 6 of Table 2 a revised classification for each galaxy. The objects having a composite spectrum (CS) are those with line ratios lying to the right of the H II region line in all 3 diagnostic-diagrams. Objects with a possible composite spectrum (CS?) are those with line ratios satisfying the above criterion in at least one diagnostic-diagram.
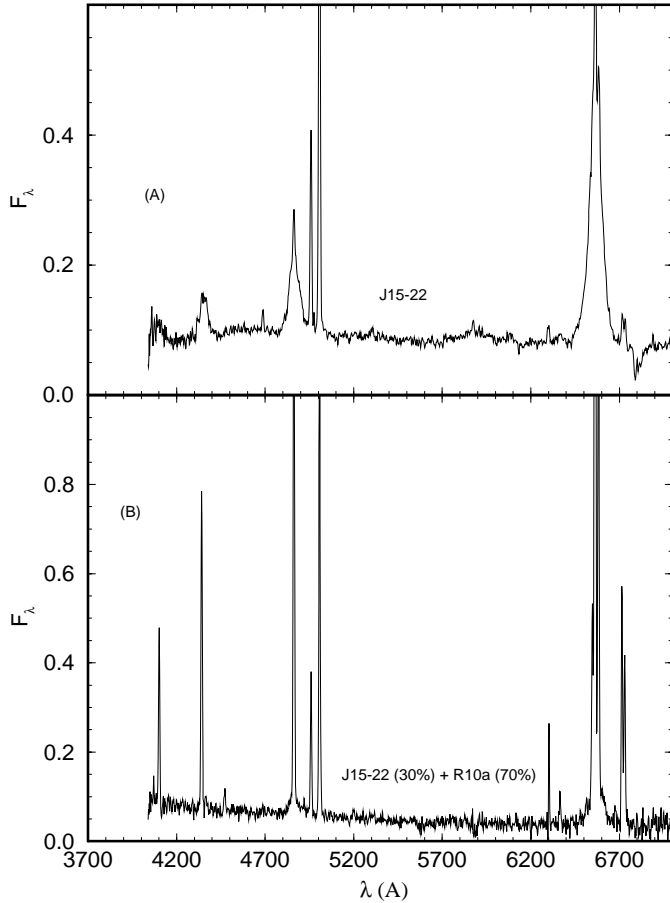
Fig. 7. (A) The Classical Seyfert 1 J 15.22. (B) Combined spectrum: 30% of J 15.22 with 70% of R10a; fractions in flux at $\lambda 5007$ Å. Spectra are plotted in F_λ units.

From this approach, we conclude that 15 objects (28% of the sample) may be **AGN** contaminated by some fraction of H II region emission due to the simultaneous presence on the slit of a Seyfert nucleus and an H II region. Including the possible composite spectra (CS?) this number is increased to 20, which corresponds to 37% of the present galaxy sample, which is consistent with previous results (Ho, Filippenko & Sargent 1997; Liu & Kennicutt 1995).

6. Conclusions

In this paper we have studied the stellar population, nuclear emission and the presence of **AGN** in a sample of 27 physical galaxy pairs. The main conclusions can be summarised as follows:

(i) The stellar population analysis based on equivalent widths of absorption lines and continuum distribution shows that about half of the bulges of the A components have a very red stellar population and solar abundance, while more than 70% of the B components have an important flux contribution at $\lambda 5870$ Å from populations younger than 10^8 years. From this we infer that the interaction induces strong star formation on the smaller component of the pairs. The effect of interac-

tion is also apparent from the tidal distortions observed in the B components.

(ii) From the usual diagnostic-diagrams, we observed that almost all galaxies have emission line-ratios typical of H II region spectra. However, we noticed that many of these line-ratios are found very close to the transition zone between H II regions and LINERs. In fact, the $[OIII]_{\lambda 5007}/H\beta \times [OI]_{\lambda 6300}/H\alpha$ diagram, which is a good indicator of LINER-like emission line spectra, shows that 4 LINERs and 1 Seyfert 2 galaxy are present in our sample. This number corresponds to 9.2% of the galaxies in our sample.

(iii) We investigated the possible nature of the galaxies with line ratios in the transition zone between H II regions and **AGN** assuming that these objects could have a composite spectrum due to the simultaneous presence on the slit of a Seyfert nucleus and an H II region. To test this hypothesis we built composite spectra contaminating emission-pure **AGN** spectra with H II regions of solar abundance. We found that this model applies to 15 objects (and possibly 5 others) in our sample, indicating that they might host a low-luminosity **AGN**. The true nature (LINER or type 1 and 2 Seyfert) of the **AGN** can only be revealed through high spatial resolution spectroscopy. It is interesting to point out that both components of the pairs AM 1118-350, AM 1304-333, AM 2229-735 and AM 2322-821 possibly host a low-luminosity active nucleus.

References

Bica E., 1988, A&A 195, 76
Bica E., Arimoto N., Alloin D., 1988, A&A 202, 8
Bica E., Alloin D., 1986, A&A 166, 83
Bushouse H.A., 1986, AJ 91, 225
Bonatto C., Bica E., Pastoriza M.G., Alloin D., 1999, A&A, in press
Calzetti D., Kinney A.L., Storchi-Bergmann T., 1994, ApJ 429, 582
Calzetti D., Bohlin R.C., Kinney A.L., Storchi-Bergmann T., Heckman T.M., 1995, ApJ 443, 136
de Vaucouleurs G., de Vaucouleurs A., Corwin, et al., 1991, The Third Reference Catalogue of Bright Galaxies. Springer Verlag, New York, RC3
Donzelli C.J., Ferreiro D.L., 1998, A&AS 127, 527
Donzelli C.J., Pastoriza, M.G., 1997, ApJS 111, 181 (DP97)
Ferland G. J., 1993, Hazy, a Brief Introduction to CLOUDY. University of Kentucky Physics Department internal report
Girardi L.A., Bica E., Pastoriza M.G., Winge C., 1997, ApJ 486, 847 (G97)
Hernquist C., Mihos J.C., 1995, ApJ 448, 41
Ho L.C., Filippenko A., Sargent W.L.W., 1997, ApJ 487, 568
Keel W.C., Kennicutt R.C., Hummel E., van der Hulst J.M., 1985, AJ 90, 708
Kennicutt R.C., Keel W.C., van der Hulst J.M., Hummel E., Roettiger K.A., 1987, AJ 93, 1011
Liu C.T., Kennicutt R.C., 1995, ApJ 450, 547
Mccall M.L., Rybski P.M., Shields G.A., 1985, ApJS 57, 1
Maza J., Ruiz M.T., Gonzalez L.E., Wischnjewsky M., Antezana R., 1994, Rev. Mex. Astro. Astrofis. 28, 187

Osmer P.S., Smith M.G., Weedman D.W., 1974, ApJ 192, 279

Osterbrock D.E., 1989, In: Astrophysics of Gaseous Nebulae and Active Galactic Nuclei. University Science Books, Mill Valley, CA

Pastoriza M.G., Dottori H.A., Terlevich E., Terlevich R., Diaz A., 1993, MNRAS 260, 177

Phillips M.M., Charles P.A., Baldwin J.A., 1983, ApJ 266, 485

Rola C.S., Terlevich E., Terlevich R.J., 1997, MNRAS 289, 419

Schild R.E., 1977, AJ 82, 337

Sérsic J.L., Pastoriza M.G., 1967, PASP 79, 152

Storchi-Bergmann T., Rodríguez-Ardila A., Schmitt H.R., Wilson A.S., Baldwin J. A., 1996a, ApJ 472, 83

Storchi-Bergmann T., Wilson A.S., Baldwin J.A., 1996b, ApJ 460, 252

Veilleux S., Kim D.C., Kron R.G., 1995, ApJ 435, L105

Veilleux S., Osterbrock D.E., 1987, ApJS 63, 295

Veron P., Goncalves A.C., Veron-Cetty M.P., 1997, A&A 319, 52 (V97)